Journal of Inflammation Research

Dovepress
open access to scientific and medical research

Open Access Full Text Article

ORIGINAL RESEARCH

Interactions of Fibroblast Subtypes Influence Osteoclastogenesis and Alveolar Bone Destruction in Periodontitis

Haicheng Wang[1,*], Renbin Wang[2,*], Jingwen Yang[3–5], Yuan Feng[6], Shuyu Xu[6], Qing-Guo Pei[7]

[1]Department of Pathology, School & Hospital of Stomatology, Tongji University, Shanghai Engineering Research Center of Tooth Restoration and Regeneration, Shanghai, 200072, People's Republic of China; [2]Department of Gastroenterology, The People's Hospital of Zhongjiang, Zhongjiang, Sichuan Province, 618100, People's Republic of China; [3]Department of Prosthodontics, Peking University School and Hospital of Stomatology, Beijing, 100081, People's Republic of China; [4]National Center of Stomatology & National Clinical Research Center for Oral Diseases, Beijing, 100081, People's Republic of China; [5]National Engineering Research Center of Oral Biomaterials and Digital Medical Devices, Beijing, 100081, People's Republic of China; [6]Department of Oral Implantology, School of & Hospital Stomatology, Tongji University, Shanghai Engineering Research Center of Tooth Restoration and Regeneration, Shanghai, 200072, People's Republic of China; [7]Department of Stomatology, Shanghai General Hospital, Shanghai Jiao Tong University School of Medicine, Shanghai, 200080, People's Republic of China

*These authors contributed equally to this work

Correspondence: Shuyu Xu, Department of Oral Implantology, School of & Hospital Stomatology, Tongji University, Shanghai Engineering Research Center of Tooth Restoration and Regeneration, 399 Yanchang Road, Shanghai, 200072, People's Republic of China, Tel +86-21-66313725/(8610); +8618616308949, Email shuyu_xu0809@163.com; Qing-Guo Pei, Department of Stomatology, Shanghai General Hospital, Shanghai Jiao Tong University School of Medicine, 100 Haining Road, Hongkou District, Shanghai, 200080, People's Republic of China, Tel +86-21-37798330/(8610); +8613764521025, Email dentistpei@126.com

Background: To analyze the fibroblasts subtypes in the gingival tissues of healthy controls, gingivitis and periodontitis patients, as well as the effects of interaction between subtypes on alveolar bone destruction.

Methods: Gingival tissues were divided into three groups according to clinical and radiographic examination, and the immunostaining of EDA+FN was assessed. Fibroblasts from gingiva developed colony formation units (CFUs) and induced Trap+MNCs. The expression of osteoclastogenesis-related genes was assessed by real-time PCR. Variances in the gene profiles of CFUs were identified by principal component analysis, and cluster analysis divided CFUs into subtypes. The induction of Trap+MNCs and gene expression were compared among individual or cocultured subtypes. The fibroblast subtypes exerted critical effect on Trap+MNCs formation were selected and edited by CRISPR/Cas to investigate the influence on osteoclastogenesis in the periodontitis in mice.

Results: Most periodontitis samples exhibited intensive EDA+FN staining ($P < 0.05$), and these fibroblasts also induced most Trap+MNCs among three groups; consistently, fibroblasts from periodontitis highly expressed genes facilitating osteoclastogenesis. According to gene profiles and osteoclastogenic induction, four clusters of CFUs were identified. The proportion of clusters was significantly different ($P < 0.05$) among three groups, and their interaction influenced osteoclastogenic induction. Although Cluster 4 induced less osteoclasts, it enhanced the effects of Clusters 1 and 3 on Trap+MNCs formation ($P < 0.05$). EDA knockout in Cluster 4 abrogated this promotion ($P < 0.05$), and decreased osteoclasts and alveolar bone destruction in experimental periodontitis ($P < 0.05$).

Conclusion: Heterogeneous fibroblast subtypes affect the switch or development of periodontitis. A subtype (Cluster 4) played important role during alveolar bone destruction, by regulating other subtypes via EDA+FN paracrine.

Keywords: periodontitis, heterogeneity, fibroblast subtype, osteoclastogenesis, alveolar bone destruction

Introduction

Both gingivitis and periodontitis are microbial-initiated inflammation in periodontal tissues, exhibiting bleeding on probing (BOP) or increased probing depth (PD). Most gingivitis is confined to gingival tissues without destroying tooth-supporting structures,[1] but some gingivitis further develops into periodontitis, leading to clinical attachment loss (CAL)

Received: 10 May 2023
Accepted: 18 July 2023
Published: 25 July 2023

and alveolar bone destruction.[2] However, it is unclear why some gingivitis readily develops into periodontitis and others remain stable for several years even though the patients' general health is similar.[2,3]

The cellular components of inflammation influence the switch and development of periodontitis.[4,5] For instance, innate lymphoid 1 cells (ILC1s) and $CD138^{+}HLA^{-}DR^{low}$ plasma cells, which express receptor activator of NF-κB ligand (RANKL), predominate in periodontitis but not gingivitis;[2,6] and triggering receptor expressed on myeloid cells 2 (TREM-2)-positive cells, which can be induced to osteoclasts by RANKL, also increase as alveolar bone destruction is exacerbated.[5] These cell subtypes express different genes related to osteoclastogenesis, and changes in their proportions tend to participate in the switching or development of periodontitis because alveolar bone destruction is a criterion for distinguishing gingivitis and periodontitis.[1,2] Under pathological conditions, interactions with inflammatory cells, cytokines or abnormal extracellular matrix (ECM) always diversify gene profiles in fibroblasts,[7,8] and the microenvironment of gingivitis and periodontitis may also facilitate such cellular heterogeneity.[9]

In our previous studies,[10–14] we reported that in the odontogenic cysts, microenvironment components endued fibroblasts with different gene expression and effects on osteoclastogenesis, suggesting associations between fibroblast subtypes and bone destruction. Subsequently, within the connective tissue of radicular cysts, which are also initiated by chronic inflammation, fibroblast subtypes have been identified, by statistically clustering colony formation units (CFUs)[15] according to the expression of a series of osteoclastogenesis-related genes, including COX-2, IL-6, IL-17, M-CSF, IL-1α, TNF-α, RANKL, OPG and VEGF-A,[12,13] as well as inflammation-specific fibronectin isoforms.[16] Under the inflammatory condition of radicular cysts, the fibroblast subtype highly expressing the fibronectin isoform, EDA+FN, was demonstrated to be principal subtype promoting bone destruction,[15] and knockout of the EDA exon decreases the expression of osteoclastogenesis-related cytokines;[12–14] consequently, EDA knockout decreases the proportion of this fibroblast subtype, thereby attenuating jawbone destruction.[15]

During periodontitis, various mediators, such as TGF-beta 1 or VEGF,[17] serve as inflammatory microenvironment to promote the splicing of EDA exon,[18] and change the miRNAs profiles in gingival tissues as well,[19] facilitating the generation of fibroblast subtypes expressing distinct osteoclastogenesis-related gene profiles.[1,15] According to the ratio or interaction between subtypes, the present study aim to identify a critical subtype which endue other subtypes with osteoclastogenic effects, leading to alveolar bone destruction. Based on intermediary molecule between subtypes, it may be helpful to attenuate the development of periodontitis, as described previously.[20]

Materials and Methods

Collection of Gingival Tissue Specimens

As described in our previous study,[5] the gingival tissues of chronic periodontitis, gingivitis and clinically healthy gingiva were collected. The inclusion criteria were as follows: (a) At least 18 years old; (b) Had good general health. The exclusion criteria were as follows: (a) Present decompensated metabolic disease, pregnancy, metabolic bone diseases or treatment with radiotherapy in the last five years; (b) Presence of acute periodontal infections; (c) Current use anticoagulant, chemotherapy drug, bisphosphonates, corticosteroids, or immunosuppressant.

The alveolar bone loss of periodontitis was confirmed by radiography, and the specimens were collected from sites of extracted teeth or periodontal surgery. The inflamed sites of gingivitis exhibited bleeding on probing but no clinical attachment or bone loss, and specimens were collected from tooth extractions due to pericoronitis. Healthy gingival tissues were collected from the sites of tooth extractions for orthodontic reasons, and there were no signs of inflammation (no bleeding on probing, probing depth ≤3 mm, no clinical attachment and no bone loss). All gingival tissue specimens were collected at the Department of Stomatology of Shanghai General Hospital and Department of Oral and Maxillofacial Surgery of TongJi University School of Stomatology (2020–2022) from patients who provided written informed consent, and this study was approved by the Review Board of TongJi University (Shanghai, China; permit number: SL2016R6 [2016]-19; February 19, 2016). The whole study complies with the Declaration of Helsinki.

According to previous studies, the probing depth (PD), clinical attachment loss (CAL), plaque index (PI) and bleeding on probing (BOP) were measured and recorded.[1,5,21] The clinical data of the patients are listed in Supplement Tables 1 and 2.

Histopathological Analysis

Each surgical specimen was divided into two parts, and one part was used for histological analysis. Specimens were fixed in formalin, embedded in paraffin and sectioned at a thickness of 4 μm for haematoxylin and eosin (H&E) and immunohistochemical staining. As described in our previous studies,[12–15] sections were incubated with IST-9 antibodies (Abcam Ltd., Cambridge, MA, USA) at 4°C overnight. To investigate the EDA+FN staining, negative controls were incubated with PBS. Sections were subsequently incubated with biotinylated secondary antibody (1:200) at 37°C for 1 h, and the immunocomplexes were visualized with diaminobenzidine (Zhongshan Golden Bridge Biological Technology Co., Ltd., Beijing, China). EDA+FN staining was visualized by microscopy (Olympus, Tokyo, Japan) and quantified with Image-Pro Plus ver. 6.0 software (Media Cybernetics, Silver Spring, MD, USA). According to the optical density, EDA +FN staining was demarcated as groups of high or low expression as in our previous studies.[15,22]

Cell Culture and Colony Forming Unit (CFU) Assay

Both the fibroblasts and Raw 264.7 cells which was purchased from Shanghai Fuheng Biotechnology Co., Ltd. (Cat No.: FH0328, Shanghai, China) were maintained at 37°C in 95% humidity and an atmosphere of 5% CO_2, and they were cultured in α-modified Eagle's medium (α-MEM) (GIBCO, Grand Island, NY, USA) containing 100 g/mL streptomycin, 100 U/mL penicillin, 2 mM L-glutamine and 10% fetal bovine serum (FBS).[5,12–15]

According to our previous studies,[10,13,15] fibroblasts were routinely isolated from the other part of the 42 surgical specimens and cultured for one passage, and the fibroblasts were then seeded into 100 mm dishes at a density of 1000 cells/dish for 14 days. Colony formation units (CFUs) containing more than 50 cells were recorded, and crystal violet was used to stain the cells. For each case, the CFU assay was performed at least once. In another set of CFU assays, fibroblasts were seeded at a density of 100 cells/dish for 14 days, and the aggregates containing more than 100 cells were digested by trypsin-EDTA and cultured in 24-well plates separately.[15,23] Only when the cell confluence reached 70% were the cells passed into dishes for further experiments. The numbers of CFUs are listed in Supplement Table 1.

Collection of Conditioned Medium for Inducing Osteoclastogenesis

When fibroblasts in 60 mm or 100 mm dishes reached a confluency of 70–80%, the medium was replaced with serum-free α-MEM and maintained for 7 days. The supernatants were then collected and centrifuged for 10 min at 550 g. For the conditioned medium, fresh α-MEM (40%, Gibco) and 10% FBS were added to the 50% aliquoted supernatant.[12–15]

Raw 264.7 cells (osteoclast precursor cells) were seeded into 24-well plates at a density of 1000 cells/well and induced by conditioned medium containing 12 ng/μL recombinant murine RANKL (R&D). Conditioned medium was refreshed at 1-day intervals for 10 days, and the cells were then stained with a tartrate-resistant acid phosphatase (TRAP) kit (Sigma, St. Louis, MO, USA). Cells containing no less than three nuclei and stained with TRAP (Trap+MNCs) were defined as osteoclast-like cells.[12–15]

The Effects of Cocultured Fibroblasts on Osteoclastogenesis and EDA Knockout

Transwell chambers with a polycarbonate membrane (Millipore, Bedford, MA, USA) were used to investigate the influence of intercellular interactions on osteoclastogenic induction. Different fibroblasts were separately cocultured in the upper or lower chamber for 48 hours. The upper chamber was removed, and the lower chamber was then replaced with serum-free α-MEM for another 5 days. The supernatants were then collected for conditioned medium, which was then used to induce osteoclastogenesis.

Fibroblasts lacking the EDA exon, which was knocked out using the same protocol as described in our previous studies,[12–15] were also used for coculture. Briefly, when the cell confluence reached 70–90%, the medium was replaced with serum-free medium. After 6 h, plasmids containing single guide (sg) RNAs that recognize the DNA flanking the EDA exon were transfected into the cells with Lipofectamine 3000 according to the manufacturer's protocol (Life Technologies, Carlsbad, CA, USA). The primer sequences and sgRNAs were identical to those described in our previous study,[14,15](Supplement Table 3).

Ligature-Induced Periodontitis and Interference of Osteoclastogenesis in vivo

As described previously,[5,24] an experimental periodontitis model was used to investigate periodontal tissue destruction. All mice were obtained from the Laboratory Animal Centre of Tongji University according to the International Guiding Principles for Animal Research (1985). Before surgery, the mice were acclimatized to animal housing facility cages, fed a standard laboratory diet and housed at ambient temperature and humidity. The experimental protocol was approved by the Laboratory Animal Centre of Tongji University (No. [2019]-DW-017).

Mice were anesthetized with 3% sodium pentobarbital, and a 9-0 silk suture was placed in the gingival sulcus around the left first mandibular molar. According to our previous studies,[5,15] the mice were divided into three groups as follows: untreated control group, in which 10 μL of physiological saline was injected into the gingiva; and EDA knockout group, in which EDA knockout fibroblasts (1×10^5) were resuspended in physiological saline and injected into the gingiva; in addition, mice injected with untreated fibroblasts were taken as positive control. On the Days 3 and 7 after ligature placement, the mice were euthanized, and the maxillae were harvested for further analysis.

Micro-CT Analysis of Bone Volume in the Furcation Area and Alveolar Bone Loss

Mandibles were scanned with a micro-CT instrument (micro-CT35, Scanco Medical AG, Bassersdorf, Switzerland) with a 15 μm voxel size with the following conditions: 114 mA, 70 kVp and 300 ms exposure time. The software accompanying the micro-CT machine was used to reconstruct the scanned images and further produce 3D microarchitectures. As described previously,[25] the area of remaining bone volume was determined between the mesial and distal root of the first molar according to the region of interest (ROI) in micro-CT 2D sagittal sections. In addition, the alveolar bone loss was determined by the area of the lingual root surfaces of the first mandibular molar as well as the distance from cemento-enamel junction to alveolar bone crest on the mesial, middle and distal regions of the first mandibular molar. The area and depth were measured using Image-Pro Plus ver. 6.0 software (Media Cybernetics, Silver Spring, MD, USA).

RNA Extraction, Reverse Transcription and PCR Amplification

Total RNA (2 μg) extracted with TRIzol Reagent (Life Technologies) was reverse-transcribed into cDNA by a superscript first-strand synthesis kit (Life Technologies). Real-time PCR (20 μL mixture per sample) was performed with 4 replicates for each gene using the primers listed in Supplement Table 4. A LightCycler real-time PCR system (Roche Diagnostics Ltd., Shanghai, China) was used with the following thermocycler program: 95°C for 10 min; and 40 cycles of annealing/extension at 60°C for 1 min and denaturation at 95°C for 15 sec. The relative expression of FN isoforms and osteoclastogenesis-related genes was assessed and normalized to human β-actin.

Statistics

Quantitative data are presented as the mean ± standard deviation (SD). Among three or more groups, differences were assessed using one-way ANOVA with repeated measures followed by the LSD or Tamhane's multiple comparison test. The differences between two groups were evaluated using Student's *t*-test as described in our previous study.[15] According to EDA+FN staining, clinicopathological specimens were divided into groups and evaluated with chi-square tests. Statistical significance was set at $P<0.05$. SPSS version 20.0 software (SPSS Inc., Chicago, USA) was used to perform statistical analyses. Each experiment was performed in triplicate.

According to previous studies,[15,26] principal component analysis (PCA) was used to evaluate the characteristics of each CFU based on assessed FN isoforms and osteoclastogenesis-related genes. Each measured value was normalized for use in PCA. Components exhibiting eigenvalues ≥1.0 were considered as principal components (PCs). In the automated population separator (APS) view, as a linear combination of parameters with distinct statistical weights, different PCs represented each axis of a plot, and the selected clusters were compared with each other to identify significantly different bins in search of cellular subtypes.[27]

Results

Clinical Characteristics of Patients

The 42 individuals consisted of 21 females and 21 males, and each sample was divided into two parts for immunohistochemistry and fibroblast isolation. The mean ages were 39.4±7.6 years in the healthy group, 43.9±11.2 years in the gingivitis group and 51.0±10.4 years in the periodontitis group. The site-specific clinical parameters are presented using the median and interquartile range in Supplement Table 2.

Histological and Radiographic Investigation of Periodontal Tissues

As illustrated by panoramic radiographs (Figure 1A), the teeth of healthy controls and gingivitis patients retained intact alveolar bone, and lamina dura surrounded the tooth root; however, in periodontitis teeth, the lamina dura disappeared, and the interdental septa loss was obvious, indicating alveolar bone destruction.[28]

In the connective tissue adjacent to the gingival epithelium, the inflammatory infiltration was similar between the gingivitis and periodontitis groups (Figure 1B), which was consistent with previous studies.[5,29] According to the median staining intensity of EDA+FN (IOD/μm^2=49), the samples were divided into groups of low and high EDA+FN expression. Most periodontitis samples belonged to the group with high EDA+FN expression (72.22%), and this percentage was significantly higher than that in the healthy control (χ^2=4.6796, P = 0.0305) and gingivitis (χ^2=4.2651, P = 0.0389) groups (Table 1) (Figure 1C).

Comparison of Osteoclastogenic Induction and Gene Expression Among Three Groups

Fibroblasts isolated from periodontitis induced significantly more Trap+MNCs (10.0357±6.9910/well) than healthy controls (5.1833±4.2402/well, P = 0.0163), but the differences between the groups of gingivitis (8.4545±6.4238/well) and periodontitis (P = 0.8261) or healthy controls (P = 0.1250) were insignificant (Figure 1D and E). Although the difference in EDA+FN expression was insignificant, the expression of other osteoclastogenesis-related genes in fibroblasts from the periodontitis group was highest among the three groups, including COX-2, IL-6, MCSF, IL-1α, TNF-α, VEGF-A and RANKL as well as RANKL/OPG ratio (Supplement Table 5) (Figure 1F and G), which was also consistent with the osteoclastogenic induction of these fibroblasts.[30]

Cluster Analysis of the CFUs Based on Principal Component Analysis (PCA)

Each aggregation of colony-forming units (CFUs) contained more than 50 cells, which displayed well spread, spindle-shaped and elongated fibroblast-like appearance[10] (Figure 2A). The numbers of CFUs developed from fibroblasts in healthy controls (n = 10, 63.6100±23.3557/1000 cells), gingivitis patients (n = 14, 71.5000±21.6147/1000 cells) and periodontitis patients (n = 18, 69.2000±15.8606/1000 cells) were approximately equal (Figure 2B). Fifteen CFUs from healthy controls, 22 CFUs from gingivitis and 25 CFUs from periodontitis groups have survived for the subsequent osteoclastogenic induction assay.

As described in previous studies,[15,27] principal component analysis (PCA) allowed analysis of entire profiles of our assessed osteoclastogenesis-related genes in fibroblasts from each CFU (Figure 2C and D). Principal components (PCs) with eigenvalues ≥1 were calculated to examine the variations in the fibroblast CFUs as described previously.[26] In the present study, PC1, PC2 and PC3 accounted for 53.0272%, 11.3542% and 10.5885% of the variance among CFUs, respectively (Supplement Table 6). According to the median position of individual CFUs in the coordinate analysis of PC1, PC2 and PC3, the CFUs were divided into four clusters (Clusters 1, 2, 3 and 4) representing distinct profiles of our assessed osteoclastogenesis-related genes (Figure 2E). Gingivitis and periodontitis had only 2 CFUs in Cluster 2, which was absent in healthy controls, and the percentages of Clusters 1, 3 and 4 were significantly different among the three groups (Supplement Table 7). Most CFUs from healthy controls were Cluster 1 (86.67%), and the number of CFUs in Clusters 3 and 4 was increased in the gingivitis and periodontitis groups (Supplement Table 8).

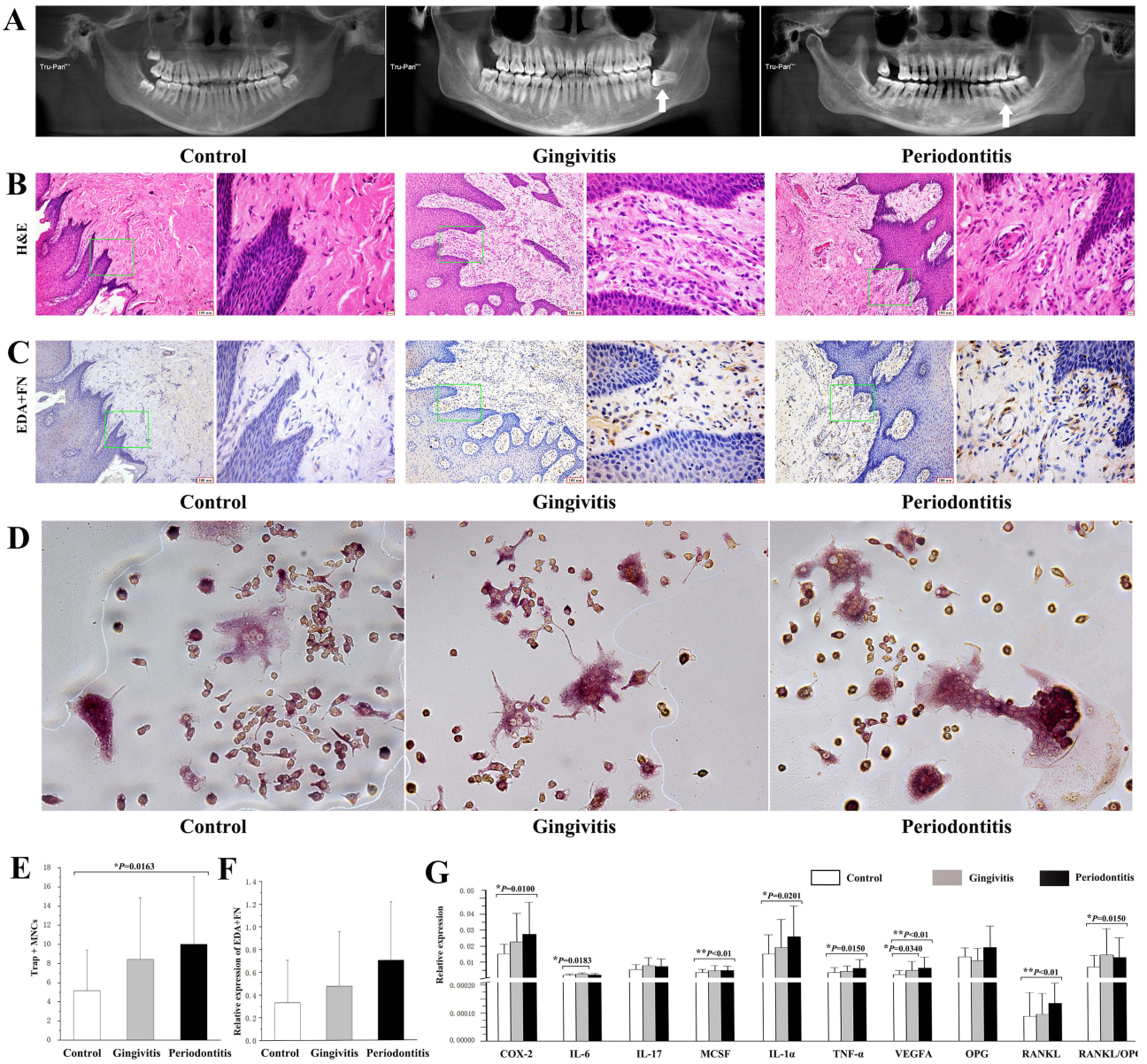

Figure 1 Radiographic, histological and cellular characteristics of healthy controls, gingivitis patients and periodontitis patients. (**A**) Panoramic radiographs of healthy control, gingivitis and periodontitis samples. (**B**) Hematoxylin and eosin staining of gingival tissues (original magnification ×100, scale bar = 100 μm; local magnification ×400, scale bar = 10 μm). (**C**) Comparison of EDA+FN expression among different gingival tissues (original magnification ×100, scale bar = 100 μm; local magnification ×400, scale bar = 10 μm). (**D**) The Trap+MNCs induced by fibroblasts isolated from the healthy control, gingivitis and periodontitis groups (original magnification of ×200, scale bar = 50 μm). (**E**) Comparison of Trap+MNCs induced by fibroblasts among the three groups. (*P < 0.05) (**F**) Relative expression of EDA+FN among the three groups. (**G**) Relative expression of other osteoclastogenesis-related genes as well as the RANKL/OPG ratio among the three groups. (*P < 0.05; **P < 0.01).

Comparison of the Osteoclastogenic Induction and Gene Expression Among Clusters

The fibroblasts in Cluster 2 induced the most Trap+MNCs (n = 4, 20.3750±2.9288/well) among the four clusters, and the fibroblasts in Cluster 3 induced more Trap+MNCs (n = 14, 16.1964±4.5407/well) than those in Clusters 1 (n = 26, 4.2981 ±3.1241/well, P < 0.0001) and 4 (n = 21, 5.9405±3.1650/well, P < 0.0001) (Figure 3A and B). In Cluster 2, the increased expression of EDA+FN and a series of osteoclastogenic genes was consistent with effective osteoclastogenic induction (Supplement Tables 9 and 10). However, the level of EDA+FN in Clusters 1 and 3 was similar but significantly lower than that in Cluster 4 (P < 0.0001) (Figure 3C). The expression of other osteoclastogenic genes was in accordance with the increased osteoclastogenic induction of Cluster 3, in which the expression of COX-2, IL-6, MCSF, IL-1α, TNF-α,

Table 1 Correlation Between EDA+FN Expression (IOD) and Periodontal Conditions

Periodontal Conditions	Low EDA+FN Expression (IOD/μm^2≤49)	High EDA+FN Expression (IOD/μm^2>49)	χ^2 value	*p*-value
Healthy gingiva **Gingivitis**	7(70.00%) 9(64.29%)	3(30.00%) 5(35.71%)	0.0857	0.7697
Healthy gingiva **Periodontitis**	7(70.00%) 5(27.78%)	3(30.00%) 13(72.22%)	4.6796	*0.0305
Gingivitis **Periodontitis**	9(64.29%) 5(27.78%)	5(35.71%) 13(72.22%)	4.2651	*0.0389

Notes: The χ^2 value among three groups is 6.4284, and *p*-value is *0.0429. *p < 0.05.

VEGF-A and RANKL as well as the RANKL/OPG ratio were highest among Clusters 1, 3 and 4 (Figure 3D) (Supplement Table 11).

Effects of Intercellular Interactions on Osteoclastogenic Induction

Because EDA+FN stimulates the expression of other cytokines,[13,15] fibroblasts of Clusters 1, 3 and 4 were cocultured with each other to investigate intercellular interactions. Cluster 1 cocultured with Cluster 4 induced significantly more Trap+MNCs (n = 4, 15.0000±2.5495/well) than Cluster 1 alone (7.7500±3.3448/well, P = 0.0245) or Cluster 1 cocultured with Cluster 3 (9.0000±3.0822/well, P = 0.0408), which suggested that Cluster 4 enhanced the effects of Cluster 1 on osteoclastogenesis. In contrast, Cluster 1 decreased the osteoclastogenic induction of Cluster 3, and Cluster 3 cocultured with Cluster 1 induced significantly fewer Trap+MNCs (n = 4, 6.5000±2.6926/well) than Cluster 3 alone (13.2500 ±3.4911/well, P = 0.0379) and Cluster 3 cocultured with Cluster 4 (16.2500±5.4486/well, P = 0.0321). However, among Cluster 4 cocultured with Cluster 1 (6.5000±2.5000/well), Cluster 4 cocultured with Cluster 3 (8.5000±2.2913/well) and Cluster 4 alone (n = 4, 6.7500±3.2692/well), the number of Trap+MNCs induced by fibroblasts was similar (P > 0.05) (Figure 3E).

To explore the role of EDA+FN in the interaction between clusters, the EDA exon was knocked out in the Cluster 4 fibroblasts. According to our previous studies,[15,22,31] the width of the band lacking the EDA exon (415 bp) exceeded the band containing the EDA exon (675 bp), which resulted in decreased EDA+FN protein levels, suggesting that the EDA exon was excluded from the majority of cells in which the total FN level remained stable (Figure 4A and B). Cluster 1 coculture with EDA knockout Cluster 4 induced significantly less Trap+MNCs (n = 6, 7.5000±2.8247/well) than Cluster 1 cocultured with untreated Cluster 4 (15.875±6.4626/well, P = 0.0241), but was similar to the Trap+MNCs induced by Cluster 1 alone (6.9583±1.6420/well) (Figure 4C and D). Cluster 3 cocultured with EDA knockout Cluster 4 also induced fewer Trap+MNCs (n = 6, 5.9583±2.8189/well) than Cluster 3 alone (16.3950±3.6918/well, P = 0.0005) and untreated Cluster 4 cultured alone (20.3333±5.4077/well, P = 0.0004) (Figure 4E and F). Consistently, EDA knockout Cluster 4 maintained relatively low levels of osteoclastogenesis-related genes in the co-cultured Clusters 1 and 3, including COX-2, IL-6, MCSF, IL-1α, TNF-α, VEGF-A, RANKL and the ratio of RANKL/OPG (Supplement Tables 12 and 13 and Figure 4G and H).

Injection of Cluster 4 Interferes with Osteoclastogenesis in vivo

According to previously reported methods,[15,32,33] EDA knockout and untreated Cluster 4 fibroblasts were injected into the gingiva of animals with experimental periodontitis.[34] The formation of Trap+ osteoclasts surrounding the interdental septa was significantly suppressed by EDA knockout cells. On Days 3 and 7 after periodontitis induction, there were significantly fewer Trap+ osteoclasts in the EDA knockout group (n = 9, 4.1111±1.8526 and 2.4444±1.1653) than the control group (6.3333±1.9437, P = 0.0379; 4.8889±2.4242, P = 0.0305), as well as the group of untreated Cluster 4 (6.7778±2.2498, P = 0.0144; 5.8889±2.5142, P = 0.0035), respectively (Figure 4I and K1–K3).

After 14 days of ligature placement, micro-CT-based analyses of the remaining bone volume in the furcation area and bone defect area as well as depth indicated that the ligature successfully induced alveolar bone loss. Remarkably, the

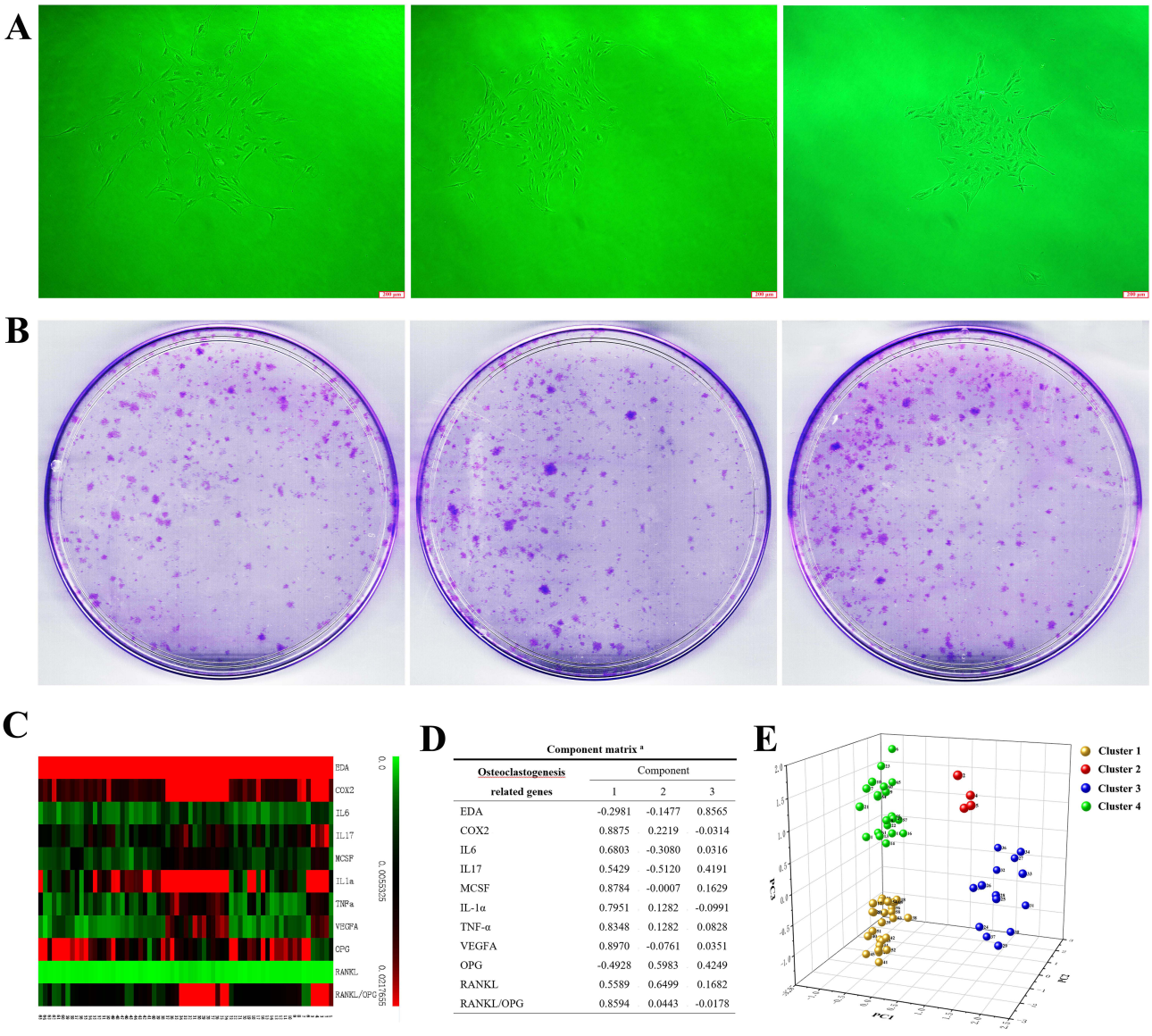

Figure 2 Clustering analysis of the colony forming units (CFUs) of fibroblasts. (**A**) The fibroblast aggregations of colony formation units (CFUs) from healthy controls, gingivitis patients and periodontitis patients (original magnification of ×40x, scale bar = 200 μm). (**B**) CFUs formed from 1000 cells isolated from the three groups. (**C**) Thermogram indicating the different expression of genes in each CFU. (**D**) Factor loading of the assessed osteoclastogenesis-related genes in PC1, PC2 and PC3. (**E**) Each pellet with a number represents the median position of its corresponding CFU in the PC1, PC2, and PC3 coordinate system, in which CFUs were divided into four clusters (yellow pellet, CFUs of Cluster 1; red pellet, CFUs of Cluster 2; blue pellet, CFUs of Cluster 3; and green pellet, CFUs of Cluster 4).

injection of EDA knockout cells significantly alleviated alveolar bone destruction, as illustrated by the decreased bone loss in the furcation and reduced area and depth of bone loss (Table 2 and Figure 4J and L).

Discussion

This study has identified 4 subtypes (Cluster 1, 2 3, 4) of fibroblasts, and the Cluster 4 expressing relatively high level of EDA+FN stimulated inflammatory factor expression in other clusters, leading to reinforced osteoclastogenesis and bone destruction. As the main component of the ECM, abnormal alternative splicing of the fibronectin (FN) gene occurs during inflammation, wound healing or tumors,[22,35] generating abnormal FN isoforms.[36] Our previous studies have demonstrated that one of the abnormal isoforms, EDA+FN, is not only increased in the inflammatory stroma of radicular cysts, but also participates in jawbone destruction by stimulating the expression of a series of osteoclastogenesis-related genes in fibroblasts.[12,13] Consistently, the present study found higher levels of EDA+FN in most periodontitis tissues

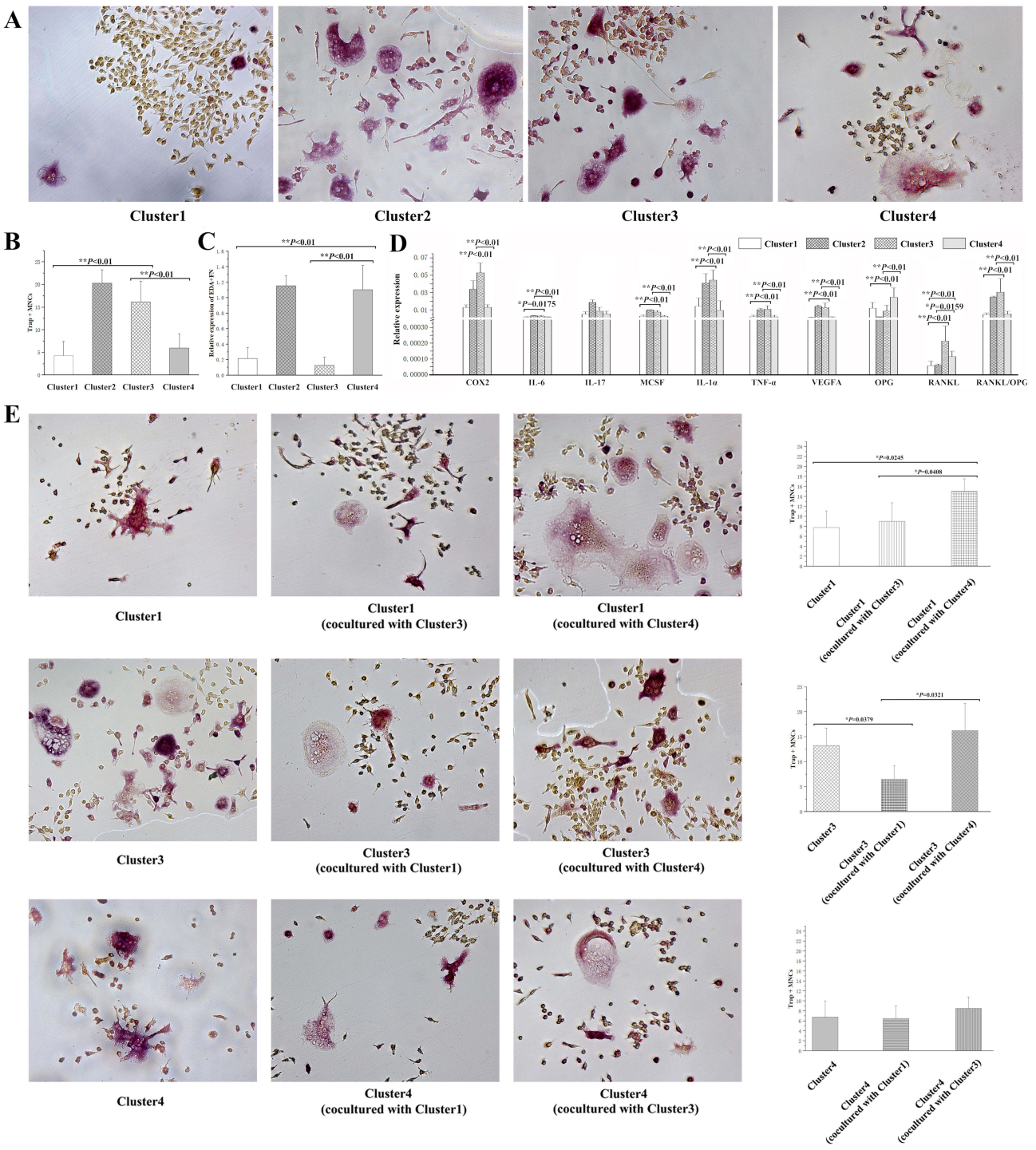

Figure 3 Osteoclastogenic induction of single cultured or cocultured clusters. (**A**) Trap+MNCs induced by fibroblasts of various clusters (original magnification of ×200, scale bar = 50 μm). (**B**) Comparison of Trap+MNCs induced by fibroblasts of different clusters. (**P < 0.01) (**C**) Relative expression of EDA+FN among the four clusters. (**P < 0.01) (**D**) Relative expression of other osteoclastogenesis-related genes as well as the RANKL/OPG ratio among Clusters. (*P < 0.05; **P < 0.01) (**E**) Comparison of the effects of intercellular interaction on the induction of Trap+MNCs by coculturing fibroblasts in which Clusters 1, 3, and 4 interacted with each other (original magnification of ×200, scale bar = 50 μm). (*P < 0.05).

compared to gingivitis and healthy gingiva tissues, suggesting effects on the development of inflammation.[28,37,38] EDA domain always facilitates the generation of inflammatory factors, including IL-1α, COX-2, VEGF-A, etc.,[39,40] through interacting with integrin containing β1 subunit;[37] therefore, the relatively high expression of EDA+FN in periodontitis also signified active bone destruction, since these factors promote osteoclastogenesis during chronic inflammations.[12,13]

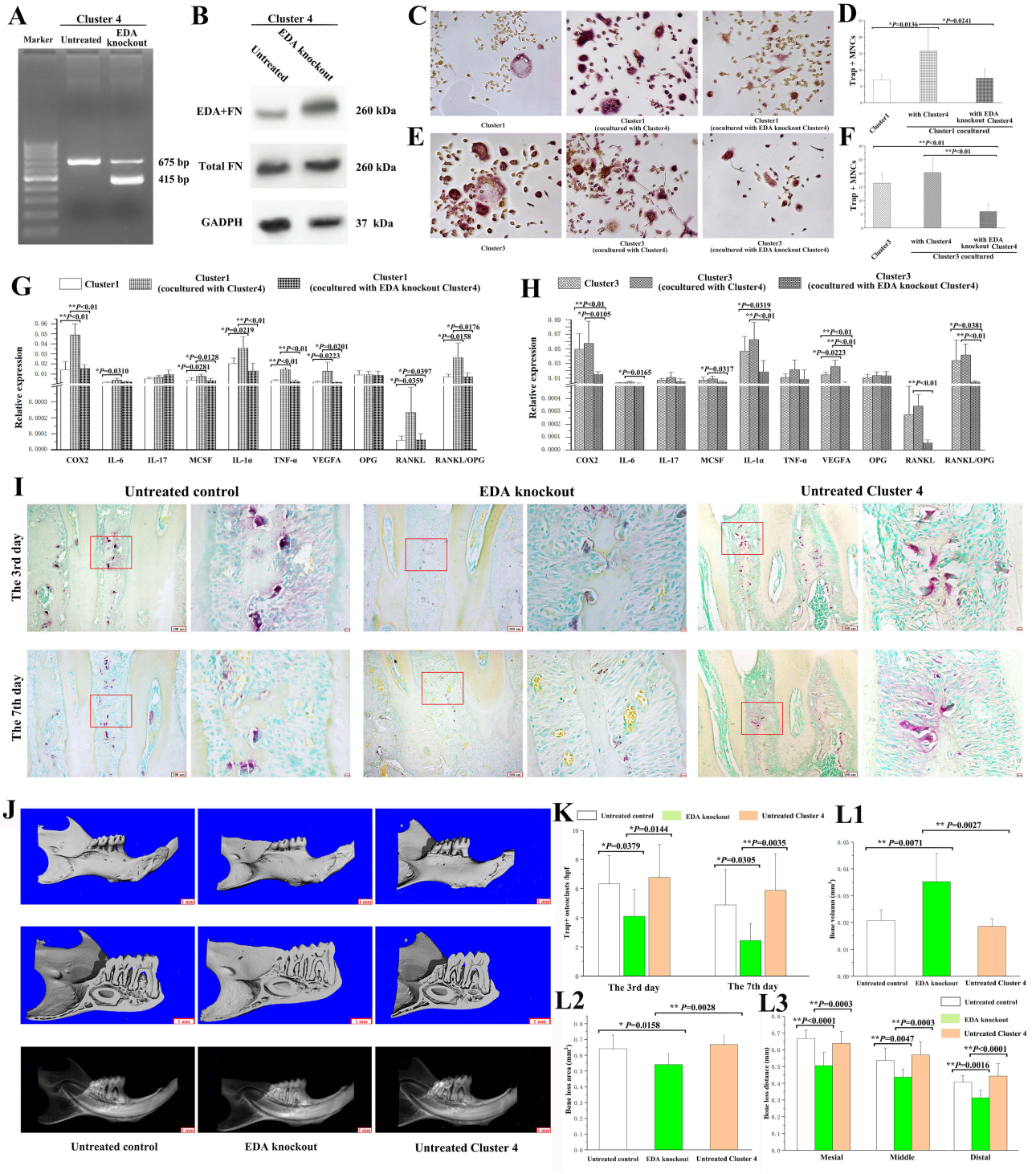

Figure 4 Effects of EDA knockout Cluster 4 on osteoclastogenic induction. (**A**) PCR product bands from EDA knockout fibroblasts of Cluster 4 (415 bp) and untreated cells (675 bp). (**B**) The protein levels of EDA+FN and total FN in EDA knockout and untreated cells were detected by Western blot analysis. (**C**) The Trap+MNCs induced by fibroblasts of Cluster 1 alone and Cluster 1 cocultured with Cluster 4 or EDA knockout Cluster 4. (original magnification of ×200, scale bar = 50 μm). (**D**) Comparison of osteoclastogenic induction among the differently cultured Cluster 1 fibroblasts. (*P < 0.05). (**E**) Trap+MNCs induced by fibroblasts of Cluster 3 alone and Cluster 3 cocultured with Cluster 4 or EDA knockout Cluster 4 (original magnification of ×200, scale bar = 50 μm). (**F**) Comparison of osteoclastogenic induction among differently cultured Cluster 3 fibroblasts. (**P < 0.01). (**G**) Relative expression of osteoclastogenesis-related genes in differently cultured Cluster 1 fibroblasts. (*P < 0.05; **P < 0.01). (**H**) Relative expression of osteoclastogenesis-related genes in differently cultured Cluster 3 fibroblasts. (*P < 0.05; **P < 0.01). (**I**) In experimental periodontitis, osteoclasts in the furcation area on Days 3 and 7 after ligature placement, including the control and EDA knockout cell groups. (**J**) Micro-CT-based analyses of remaining bone volume in the furcation area and alveolar bone loss (scale bar = 1 mm). (**K**) Comparison of the number of osteoclasts in the furcation area on Days 3 and 7 among groups. (*P < 0.05; **P < 0.01). (**L1**–**L3**) Micro-CT-based quantification of the bone volume at the furcation area, alveolar bone loss area, and depth. (*P < 0.05; **P < 0.01).

Table 2 Comparison of Bone Volume in Furcation Area and Bone Loss Area and Depth

n=10	1	2	3	*p*-value		
	Control	EDA knockout	Untreated Cluster 4	1/2	2/3	1/3
Bone volumn of furcation area (mm^3)	0.0208±0.0040	0.0353±0.0105	0.0186±0.0029	0.0071**	0.0027**	0.4966
Bone loss area (mm^2)	0.6410±0.0863	0.5416±0.0669	0.6683±0.0906	0.0158*	0.0028**	0.4859
Mesial bone loss depth (mm)	0.6672±0.0502	0.5052±0.0791	0.6388±0.0727	<0.0001**	0.0003**	0.3858
Middle bone loss depth (mm)	0.5369±0.0751	0.4371±0.0488	0.5699±0.0784	0.0047**	0.0003**	0.3166
Distal bone loss depth (mm)	0.4070±0.0409	0.3138±0.0456	0.4436±0.0753	0.0016**	<0.0001**	0.1806

Notes: *P < 0.05; **P < 0.01.

Correspondingly, fibroblasts isolated from periodontitis patients induced the highest number of osteoclasts among the healthy control, gingivitis and periodontitis groups. The enhanced osteoclastogenic induction was consistent with increased expression of osteoclastogenesis-related genes, including COX-2, IL-6, M-CSF, IL-1α, TNF-α, VEGF-A and RANKL, as well as the ratio of RANKL/OPG, in periodontitis-derived fibroblasts. Among the three groups, the difference in EDA+FN expression was insignificant, which may be attributed to bulk measurement, in which fibroblasts were mixed together, thereby mitigating the different gene expression in various subtypes. Therefore, each CFU with a distinct osteoclastogenesis-related gene profile was analyzed separately to identify various cellular subtypes as described in our previous study.[15] Because EDA+FN facilitates osteoclastogenesis by increasing the expression of other genes,[13,15] a panel of these genes in each CFU was used to cluster distinctive subtypes with similar gene profiles. Based on principal component analysis (PCA), three principal components (PC1, PC2 and PC3) accounted for the majority of the variance in colonies (74.97%); consequently, all fibroblast CFUs were divided into four clusters (1, 2, 3 and 4) using cluster analysis as described previously.[15,27]

The gingivitis and periodontitis groups had two CFUs belonging to Cluster 2, which was absent in the healthy gingiva group. Cluster 2 induced osteoclast formation as efficiently as Cluster 3 and expressed EDA+FN as high as Cluster 4; the expression of most osteoclastogenesis-related genes, such as IL6, IL17, MCSF TNF-α and VEGF-A, as well the RANKL/OPG ratio were consistently higher in Cluster 2 than in Clusters 1 or 4. The simultaneously upregulated EDA+FN and other genes in Cluster 2 suggested some similarities to our previously identified fibroblast subtype, in which highly expressed EDA+FN stimulates a series of cytokines by autocrine effects, leading to jawbone destruction in radicular cysts.[15] In Cluster 1, the relatively low EDA+FN expression was consistent with low levels of osteoclastogenesis-related genes. However, Clusters 3 and 4 exhibited contrary gene profiles because Cluster 4 expressed higher levels of EDA+FN but lower levels of osteoclastogenesis-related genes in contrast to Cluster 3, in which low EDA+FN expression was accompanied by high levels of other genes.

The osteoclastogenic induction of Cluster 4 was similar to that of Cluster 1 but lower than that of Clusters 2 and 3; however, Cluster 4 consisted of more than half of the CFUs (53.57%) from the periodontitis group, and this proportion was significantly higher than the CFUs from the healthy gingiva (6.67%) and gingivitis (22.73%) groups. These results suggested an indirect influence of Cluster 4 on osteoclast formation because EDA+FN has been demonstrated to increase the expression of cytokines.[13,15] The coculture systems in which Clusters 1, 3 and 4 interacted with each other were used to verify this speculation. The osteoclastogenic induction of Cluster 4 itself was maintained at inferior levels even when it was cocultured with Cluster 1 or 3. However, the interaction with Cluster 4 significantly increased the effects of Cluster 1 on osteoclastogenesis. In contrast, Cluster 1 significantly inhibited the osteoclastogenic induction of Cluster 3, which may be the reason why Cluster 1 consisted of 86.67% or 50.00% of the healthy gingiva- or gingivitis-derived CFUs, respectively, but only 7.14% of the periodontitis-derived CFUs. And Cluster 4 tend to be an indirect regulator from which the EDA domain interacts with integrin receptors containing β1 subunit,[37] and in turn stimulates the expression of cytokines in other clusters,[39,40] leading to alveolar bone destruction in periodontitis.[15,22,41]

EDA knockout impaired the effects of Cluster 4 on Cluster 1, leading to almost unchanged osteoclastogenic induction of Cluster 1 which cocultured with EDA knockout Cluster 4, and the osteoclastogenesis-related gene expression also remained similar between the cocultured Cluster 1 and Cluster 1 alone. Furthermore, interaction with EDA knockout

Cluster 4 attenuated the osteoclastogenic induction of Cluster 3, by decreasing the levels of COX2, IL1α, VEGF-A and RANKL as well as the RANKL/OPG ratio in Cluster 3. These results suggested that EDA+FN of Cluster 4 maintained the osteoclastogenic induction of other clusters through paracrine effects. The injection of EDA knockout cells decreased the proportion of original Cluster 4 fibroblasts in periodontitis tissues, which attenuated bone destruction as previously described,[15] thereby reflecting some effects of cell therapy.[32,42]

The present study demonstrated the effects of fibroblast subtypes on bone destruction in periodontitis, which was consistent with our previous study, showing that a fibroblast subtype promotes jawbone destruction via the autocrine effects of EDA+FN.[15] However, in the inflammatory gingiva, we identified additional fibroblast subtypes that interacted with each other via paracrine effects, which may be attributed to the increased CFU number in this study, thereby facilitating the identification of more clusters. The CFUs of Cluster 4 represented the subtype that indirectly promotes alveolar bone destruction through paracrine effects of EDA+FN on osteoclastogenesis-related genes in other fibroblast subtypes, and their interaction influences the switch and development of periodontitis.

In summary, the inflammatory microenvironment of periodontitis facilitates the generation of heterogeneous fibroblasts,[17–19] in which critical subtypes regulate the osteoclastogenesis-related gene profiles in other subtypes,[15] through the paracrine effects of EDA+FN. It may be a strategy to control pathological bone resorption, especially in implant restoration in periodontitis patients, via interfering intermediary molecules, such as miRNAs, TGF-beta 1 or EDA+FN.[17–19]

Conclusions

The fibroblasts isolated from gingiva can be divided into several subtypes, and the ratio of these subtypes influenced the switch or development of periodontitis. A critical subtype (Cluster 4) played the role of regulator and indirectly promoted alveolar bone destruction, through the paracrine effects of EDA+FN on other subtypes, in which a series of cytokines were induced and exerted osteoclastogenic induction.

Acknowledgments

This study was financially supported by grants from the National Natural Science Foundation of China (No. 82101057) and (No. 82201022); Key Research and Development Project of Hainan (No. ZDYF2021SHFZ229); Natural Science Foundation of Shanghai (No. 21ZR1469000); Hainan Provincial Natural Science Foundation of China (No. 822CXTD534); Shanghai Municipal Health Commission (No. 20204Y0096); and Songjiang District Science & Technology Commission (No. 2020SJ341).

Disclosure

The authors report no conflicts of interest in this work.

References

1. Tonetti MS, Greenwell H, Kornman KS. Staging and grading of periodontitis: framework and proposal of a new classification and case definition. *J Periodontol*. 2018;89(Suppl 1):S159–S172. doi:10.1002/JPER.18-0006
2. Kindstedt E, Koskinen Holm C, Palmqvist P, Sjostrom M, Lejon K, Lundberg P. Innate lymphoid cells are present in gingivitis and periodontitis. *J Periodontol*. 2019;90:200–207. doi:10.1002/JPER.17-0750
3. Pihlstrom BL, Michalowicz BS, Johnson NW. Periodontal diseases. *Lancet*. 2005;366(9499):1809–1820. doi:10.1016/S0140-6736(05)67728-8
4. Kurgan S, Kantarci A. Molecular basis for immunohistochemical and inflammatory changes during progression of gingivitis to periodontitis. *Periodontol 2000*. 2018;76(1):51–67. doi:10.1111/prd.12146
5. Pei QG, Wang HC, Li L, Wang ZL. Triggering receptor expressed on myeloid cells-2 stimulates osteoclast differentiation and bone loss in periodontitis. *Oral Dis*. 2022;28:1652–1661. doi:10.1111/odi.14004
6. Mahanonda R, Champaiboon C, Subbalekha K, et al. Human memory B cells in healthy gingiva, gingivitis, and periodontitis. *J Immunol*. 2016;197(3):715–725. doi:10.4049/jimmunol.1600540
7. Busch S, Andersson D, Bom E, Walsh C, Stahlberg A, Landberg G. Cellular organization and molecular differentiation model of breast cancer-associated fibroblasts. *Mol Cancer*. 2017;16(1):73. doi:10.1186/s12943-017-0642-7
8. Lambrechts D, Wauters E, Boeckx B, et al. Phenotype molding of stromal cells in the lung tumor microenvironment. *Nat Med*. 2018;24(8):1277–1289. doi:10.1038/s41591-018-0096-5
9. Raz Y, Cohen N, Shani O, et al. Bone marrow-derived fibroblasts are a functionally distinct stromal cell population in breast cancer. *J Exp Med*. 2018;215:3075–3093. doi:10.1084/jem.20180818

10. Wang HC, Li TJ. The growth and osteoclastogenic effects of fibroblasts isolated from keratocystic odontogenic tumor. *Oral Dis*. 2013;19:162–168.
11. Wang HC, Jiang WP, Sima ZH, Li TJ. Fibroblasts isolated from a keratocystic odontogenic tumor promote osteoclastogenesis in vitro via interaction with epithelial cells. *Oral Dis*. 2015;21:170–177. doi:10.1111/odi.12231
12. Wang HC, Wang P, Chen YW, Zhang Y. Bevacizumab or fibronectin gene editing inhibits the osteoclastogenic effects of fibroblasts derived from human radicular cysts. *Acta Pharmacol Sin*. 2019;40:949–956. doi:10.1038/s41401-018-0172-x
13. Liu CY, Wang HC. The fibroblast of radicular cyst facilitate osteoclastogenesis via the autocrine of Fibronectin containing extra domain A. *Oral Dis*. 2019;25:1136–1146. doi:10.1111/odi.13064
14. Yang JW, Jiang JH, Wang HC, Li CY. The extra domain A of fibronectin facilitates osteoclastogenesis in radicular cysts through vascular endothelial growth factor. *Int Endod J*. 2020;53(4):478–491.
15. Yang J, Xu S, Wang HC. Heterogeneity of fibroblasts from radicular cyst influenced osteoclastogenesis and bone destruction. *Oral Dis*. 2020;26:983–997. doi:10.1111/odi.13317
16. Lemanska-Perek A, Krzyzanowska-Golab D, Pupek M, Klimeczek P, Witkiewicz W, Katnik-Prastowska I. Analysis of soluble molecular fibronectin-fibrin complexes and EDA-fibronectin concentration in plasma of patients with atherosclerosis. *Inflammation*. 2016;39:1059–1068. doi:10.1007/s10753-016-0336-0
17. Matarese G, Isola G, Anastasi GP, et al. Immunohistochemical analysis of TGF-beta1 and VEGF in gingival and periodontal tissues: a role of these biomarkers in the pathogenesis of scleroderma and periodontal disease. *Int J Mol Med*. 2012;30:502–508. doi:10.3892/ijmm.2012.1024
18. Sapudom J, Rubner S, Martin S, Thoenes S, Anderegg U, Pompe T. The interplay of fibronectin functionalization and TGF-beta1 presence on fibroblast proliferation, differentiation and migration in 3D matrices. *Biomater Sci*. 2015;3:1291–1301. doi:10.1039/C5BM00140D
19. Isola G, Santonocito S, Distefano A, et al. Impact of periodontitis on gingival crevicular fluid miRNAs profiles associated with cardiovascular disease risk. *J Periodontal Res*. 2023;58:165–174. doi:10.1111/jre.13078
20. Isola G, Polizzi A, Iorio-Siciliano V, Alibrandi A, Ramaglia L, Leonardi R. Effectiveness of a nutraceutical agent in the non-surgical periodontal therapy: a randomized, controlled clinical trial. *Clin Oral Investig*. 2021;25:1035–1045. doi:10.1007/s00784-020-03397-z
21. Chen SS, Wang K, Zhao J, Wu WC, Wu YF, Zhao L. Increased expression of triggering receptor expressed on myeloid cells 1 and 2 in inflamed human gingiva. *J Periodontal Res*. 2017;52:512–521. doi:10.1111/jre.12417
22. Lv WQ, Wang HC, Peng J, Wang YX, Jiang JH, Li CY. Gene editing of the extra domain A positive fibronectin in various tumors, amplified the effects of CRISPR/Cas system on the inhibition of tumor progression. *Oncotarget*. 2017;8:105020–105036. doi:10.18632/oncotarget.21136
23. Zhang L, Chan C. Isolation and enrichment of rat mesenchymal stem cells (MSCs) and separation of single-colony derived MSCs. *J Vis Exp*. 2010. doi:10.3791/1852-v
24. Sima C, Aboodi GM, Lakschevitz FS, Sun C, Goldberg MB, Glogauer M. Nuclear factor erythroid 2-related factor 2 down-regulation in oral neutrophils is associated with periodontal oxidative damage and severe chronic periodontitis. *Am J Pathol*. 2016;186:1417–1426. doi:10.1016/j.ajpath.2016.01.013
25. Akiyama K, Aung KT, Talamini L, Huck O, Kuboki T, Muller S. Therapeutic effects of peptide P140 in a mouse periodontitis model. *Cell Mol Life Sci*. 2022;79(10):518. doi:10.1007/s00018-022-04537-2
26. Kawagishi-Hotta M, Hasegawa S, Igarashi T, et al. Enhancement of individual differences in proliferation and differentiation potentials of aged human adipose-derived stem cells. *Regen Ther*. 2017;6:29–40. doi:10.1016/j.reth.2016.12.004
27. Henriques A, Silva I, Ines L, et al. CD38, CD81 and BAFFR combined expression by transitional B cells distinguishes active from inactive systemic lupus erythematosus. *Clin Exp Med*. 2016;16(2):227–232. doi:10.1007/s10238-015-0348-3
28. Thorbert-Mros S, Larsson L, Berglundh T. Cellular composition of long-standing gingivitis and periodontitis lesions. *J Periodontal Res*. 2015;50(4):535–543. doi:10.1111/jre.12236
29. Takamori Y, Atsuta I, Nakamura H, Sawase T, Koyano K, Hara Y. Histopathological comparison of the onset of peri-implantitis and periodontitis in rats. *Clin Oral Implants Res*. 2017;28(2):163–170. doi:10.1111/clr.12777
30. de Moraes M, de Lucena HF, de Azevedo PR, Queiroz LM, Costa Ade L. Comparative immunohistochemical expression of RANK, RANKL and OPG in radicular and dentigerous cysts. *Arch Oral Biol*. 2011;56:1256–1263. doi:10.1016/j.archoralbio.2011.05.009
31. Wang HC, Yang Y, Xu SY, Peng J, Jiang JH, Li CY. The CRISPR/Cas system inhibited the pro-oncogenic effects of alternatively spliced fibronectin extra domain A via editing the genome in salivary adenoid cystic carcinoma cells. *Oral Dis*. 2015;21:608–618.
32. Traxler EA, Yao Y, Wang YD, et al. A genome-editing strategy to treat beta-hemoglobinopathies that recapitulates a mutation associated with a benign genetic condition. *Nat Med*. 2016;22:987–990. doi:10.1038/nm.4170
33. Liang Y, Wen L, Shang F, Wu J, Sui K, Ding Y. Endothelial progenitors enhanced the osteogenic capacities of mesenchymal stem cells in vitro and in a rat alveolar bone defect model. *Arch Oral Biol*. 2016;68:123–130. doi:10.1016/j.archoralbio.2016.04.007
34. Hu LY, Zhou Y, Cui WQ, et al. Triggering receptor expressed on myeloid cells 2 (TREM2) dependent microglial activation promotes cisplatin-induced peripheral neuropathy in mice. *Brain Behav Immun*. 2018;68:132–145. doi:10.1016/j.bbi.2017.10.011
35. Liu H, Dolkas J, Hoang K, et al. The alternatively spliced fibronectin CS1 isoform regulates IL-17A levels and mechanical allodynia after peripheral nerve injury. *J Neuroinflammation*. 2015;12(1):158. doi:10.1186/s12974-015-0377-6
36. White ES, Sagana RL, Booth AJ, et al. Control of fibroblast fibronectin expression and alternative splicing via the PI3K/Akt/mTOR pathway. *Exp Cell Res*. 2010;316(16):2644–2653. doi:10.1016/j.yexcr.2010.06.028
37. Shinde AV, Kelsh R, Peters JH, Sekiguchi K, Van De Water L, McKeown-Longo PJ. The alpha4beta1 integrin and the EDA domain of fibronectin regulate a profibrotic phenotype in dermal fibroblasts. *Matrix Biol*. 2015;41:26–35. doi:10.1016/j.matbio.2014.11.004
38. Kumra H, Reinhardt DP. Fibronectin-targeted drug delivery in cancer. *Adv Drug Deliv Rev*. 2016;97:101–110.
39. Zheng R, Varney SD, Wu L, DiPersio CM, Van De Water L. Integrin alpha4beta1 is required for IL-1alpha- and Nrf2-dependent, Cox-2 induction in fibroblasts, supporting a mechanism that suppresses alpha-SMA expression. *Wound Repair Regen*. 2021;29:597–601. doi:10.1111/wrr.12938
40. Jeong BY, Cho KH, Jeong KJ, et al. Rab25 augments cancer cell invasiveness through a beta1 integrin/EGFR/VEGF-A/Snail signaling axis and expression of fascin. *Exp Mol Med*. 2018;50:e435. doi:10.1038/emm.2017.248
41. Philippeos C, Telerman SB, Oules B, et al. Spatial and single-cell transcriptional profiling identifies functionally distinct human dermal fibroblast subpopulations. *J Invest Dermatol*. 2018;138:811–825. doi:10.1016/j.jid.2018.01.016
42. Cyranoski D. CRISPR gene-editing tested in a person for the first time. *Nature*. 2016;539(7630):479. doi:10.1038/nature.2016.20988